Analysis and Further Improvement of Fine Resolution Frequency Estimation Method From Three DFT Samples

Çağatay Candan, *Senior Member, IEEE*

***Abstract*—The bias and mean square error (MSE) analysis of the frequency estimator suggested in [1] is given and an improved version of the estimator, with the removal of estimator bias, is suggested. The signal-to-noise ratio (SNR) threshold above which the bias removal is effective is also determined.**

***Index Terms*—Cramer–Rao bound, frequency estimation, threshold effect.**

I. Introduction

THE frequency estimation method suggested in [1] is revisited by analytically characterizing the estimator bias and mean square error (MSE). Using the results of the bias analysis, a simple bias-removal stage is proposed to eliminate the effect bias on the estimator studied in [1].

Frequency estimation of complex exponential signals observed under additive white Gaussian noise is a fundamental problem of statistical signal processing naturally emerging in many applications. In [1], a frequency estimation method with two stages, namely coarse and fine frequency estimation stages, is described. In the coarse estimation stage, N-point Discrete Fourier Transform (DFT) of the input is calculated and the DFT bin with the maximum magnitude and its immediate left and right neighbors are detected. In the fine estimation stage, the complex valued outputs of the bins detected in the first stage are substituted in the following relation

$$\hat{\delta} = \frac{\tan(\pi/N)}{\pi/N}\text{Real}\left\{\frac{R[k_p-1]-R[k_p+1]}{2R[k_p]-R[k_p-1]-R[k_p+1]}\right\} \quad (1)$$

to generate the fine frequency estimate. Here, k_p is index of the DFT bin detected in the first stage having the peak magnitude. By combining the results of two stages, we can write the final frequency estimate as $(k_p+\hat{\delta})$ with the units of DFT bins or $f=(k_p+\hat{\delta})/N$ in terms of the normalized frequency (see Fig. 1).

The estimator given in (1) is the bias-corrected version of the estimator suggested by Jacobsen, [2]. In [1], a derivation for the Jacobsen estimator for small δ is provided and a bias-correction term, which is the multiplier $c_N=\tan(\pi/N)/(\pi/N)$ appearing in (1), is suggested to improve the performance. In this letter, we further extend the analysis by characterizing the bias and MSE of the estimator and suggest a bias-removal stage, following the correction stage, significantly improving the performance at high SNR.

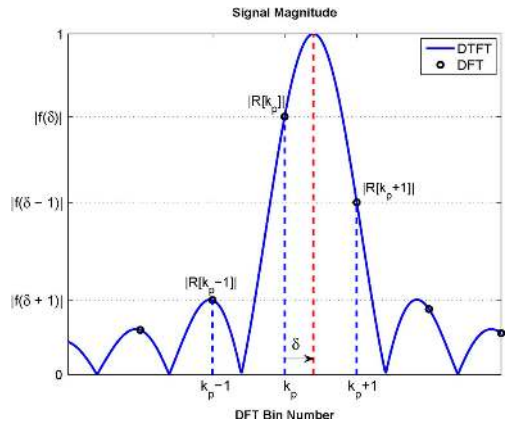

Fig. 1. A typical first stage output of the examined method in the absence of noise.

II. Preliminaries

A complex exponential signal of unknown amplitude, phase and frequency is observed under white Gaussian noise:

$$r[n]=Ae^{j(2\pi fn+\phi)}+w[n], \quad n=\{0,\ldots,N-1\}. \quad (2)$$

The frequency variable f in (2) is the normalized frequency defined in $[0,1)$. In the present work, the frequency is also denoted in terms of the DFT bins, that is $f=(k_p+\delta)/N$ where k_p is an integer in $[0,N-1]$ and δ is a real number in $-1/2<\delta<1/2$. It is assumed that noise $w[n]$ is circularly symmetric complex valued Gaussian noise with zero mean and σ_w^2 variance, $w[n]\sim\mathcal{CN}(0,\sigma_w^2)$. The signal-to-noise ratio (SNR) definition used in this work is the input SNR which is $\text{SNR}=A^2/\sigma_w^2$.

The maximum likelihood (ML) frequency estimator is known to be the periodogram, ([3], p. 539). Typically, the periodogram search is implemented by calculating a large point Fast Fourier Transform (FFT) and searching for the maxima in the magnitude spectrum. For sufficiently high number of FFT points, the error variance of the periodogram estimate is expected to approach the Cramer–Rao (CR) bound, $\text{var}(\hat{f}) \geq \frac{6}{(2\pi)^2\text{SNR}N(N^2-1)}$, ([3], eq. (15.72)), as SNR increases.

The two-stage method described in [1] calculates the N-point DFT of $r[n]$ and then a peak search in the magnitude spectrum is conducted. This stage aims to estimate the coarse part

Manuscript received June 23, 2013; accepted July 01, 2013. Date of publication July 17, 2013; date of current version July 23, 2013. The associate editor coordinating the review of this manuscript and approving it for publication was Prof. Vincenzo Matta.

The author is with the Department of Electrical and Electronics Engineering, Middle East Technical University (METU), Ankara, Turkey (e-mail: ccandan@metu.edu.tr).

Color versions of one or more of the figures in this paper are available online at http://ieeexplore.ieee.org.

Digital Object Identifier 10.1109/LSP.2013.2273616

of the frequency (k_p) as shown in Fig. 1. In the second stage, the fractional part of the frequency (δ) is estimated. Since $f = (k_p + \delta)/N$, the CR bound for the estimation of δ, or equivalently the CR bound for estimation of frequency f in terms of DFT bins, becomes

$$\mathrm{CR-Bound} = \frac{6}{(2\pi)^2 N \mathrm{SNR}}, \quad \text{for } N \gg 1. \tag{3}$$

III. Main Results

Bias for Noiseless Case: The estimator given by (1) can be expressed as $\hat{\delta} = c_N \mathrm{Real}\{B/C\}$ where $B = R[k_p - 1] - R[k_p + 1]$ and $C = 2R[k_p] - R[k_p - 1] - R[k_p + 1]$. In the absence of noise, the N-point DFT of the input $r[n] = Ae^{\phi}e^{j(2\pi f n)}$ with the frequency $f = (k_p + \delta)/N$ becomes

$$R[k_p + k] = \frac{K}{\exp\left(j\frac{\pi}{N}(\delta - 2k)\right) - \exp\left(-j\frac{\pi}{N}\delta\right)} \tag{4}$$

where $K = j2Ae^{j\phi}\exp(j\pi\frac{N-1}{N}\delta)\sin(\pi\delta)$. Using elementary complex algebra, B and C appearing in the relation $\hat{\delta} = c_N \mathrm{Real}\{B/C\}$ can be written as follows:

$$\begin{aligned} B &= \frac{2Ae^{j\phi}e^{j\pi\delta}\sin(\pi\delta)\sin(2\pi/N)}{\cos(2\pi\delta/N) - \cos(2\pi/N)}, \\ C &= \frac{4Ae^{j\phi}e^{j\pi\delta}\sin(\pi\delta)\cos(\pi\delta/N)\sin^2(\pi/N)}{\sin(\pi\delta/N)(\cos(2\pi\delta/N) - \cos(2\pi/N))}. \end{aligned} \tag{5}$$

The output of the Jacobsen estimator in the absence of noise is B/C. We denote this ratio as $\bar{\delta}_j$:

$$\bar{\delta}_j = \frac{B}{C} = \tan(\pi\delta/N)\frac{\sin(2\pi/N)}{2\sin^2(\pi/N)}. \tag{6}$$

Since $\bar{\delta}_j \neq \delta$, the Jacobsen estimator is biased even in the absence of noise. The estimator given by (1) is the bias-corrected version of the Jacobsen estimator. The correction is achieved via the multiplication of (6) by $c_N = \tan(\pi/N)/(\pi/N)$:

$$\bar{\delta}_c = \frac{\tan(\pi\delta/N)}{\pi/N} = \delta + \frac{1}{3}\left(\frac{\pi}{N}\right)^2\delta^3 + \frac{2}{15}\left(\frac{\pi}{N}\right)^4\delta^5 + \ldots \tag{7}$$

Here, $\bar{\delta}_c$ is the bias value after the correction which can be approximated with $\delta^3\pi^2/(3N^2)$ for $N \geq 8$.

SNR Value for Which Bias Meets Cramer–Rao Bound: It is well known that $\mathrm{MSE} = (\mathrm{bias})^2 + \mathrm{var}(\mathrm{error})$, [3]. Since the CR bound decreases with SNR; the bias of an estimator, however small, is expected to dominate the MSE at sufficiently high SNR. By equating the CR bound in (3) to $(\mathrm{bias})^2$, we can get the following expression for the SNR threshold:

$$\mathrm{SNR}_T^b = 27N^3/(2\pi^6\delta^6). \tag{8}$$

If the operating SNR exceeds SNR_T^b, the estimator bias is expected to be the dominant term contributing to the MSE.

MSE—General Discussion: The MSE of a non-linear estimator is significantly dependent on the input SNR. Typically, there exists three operational regions, ([4], p.21). In the low SNR region, the observations are not "useful" and do not contribute towards the reduction of MSE. This region is called no-information region. Contrary to this region, when SNR is high; MSE is solely determined by the fine estimation errors and typically follows the CR bound. The threshold region lies in between these two regions. In the threshold region, the MSE dramatically improves with a few decibels of signal power. The SNR threshold of an estimator, the SNR above which good performance is essentially guaranteed, is critical in many applications, ([4], p.21).

Specific to the frequency estimator examined in this letter, the region of no-information is the values of SNR for which the first stage fails. It is clear from Fig. 1 that when the peak detected in the first stage is at least one bin away from the true bin; the estimation error can not reduced to a value less than 1/2 bins. In this letter, we call such errors as gross errors. The fine error region of the suggested estimator is formed with the selection of the true DFT bin in the first stage. In this region, the estimator MSE is expected to approach the CR bound as SNR increases.

In this letter, we analytically characterize the fine and gross error performances of the suggested estimator and then proceed with the estimation of the SNR threshold separating these two regions.

MSE—Fine Error Characterization: The DFT of the collected samples, $R[k] = \mathrm{DFT}\{r[n]\}$, is Gaussian distributed with a non-zero mean (due to the presence of non-random signal term) and variance $N\sigma_w^2$. Furthermore, since the rows of the DFT matrix are orthogonal to each other; the random variables $R[k]$ for $k = \{0, \ldots, N-1\}$ are independent from each other.

The frequency estimate $\hat{\delta}$ given in (1) can be expressed as $\hat{\delta} = c_N \mathrm{Real}(\alpha/\beta)$. The random variables α and β denote the numerator and the denominator of the ratio in (1). Using independence of $R[k]$, it can be easily verified that α and β are independent, Gaussian distributed random variables with means B and C, with the values given in (5), and variances $2N\sigma_w^2$ and $6N\sigma_w^2$, respectively. Given these, the estimate $\hat{\delta}$ can be expressed as follows:

$$\begin{aligned} \hat{\delta} &= c_N \mathrm{Real}\left\{\frac{\alpha}{\beta}\right\} = c_N \mathrm{Real}\left\{\frac{B + w_\alpha}{C + w_\beta}\right\} \\ &= c_N \mathrm{Real}\left\{\frac{B/C + w_\alpha/C}{1 + w_\beta/C}\right\} = c_N \mathrm{Real}\left\{\frac{\bar{\delta}_j + \hat{w}_\alpha}{1 + \hat{w}_\beta}\right\} \end{aligned} \tag{9}$$

In the final equality of (9), $\tilde{w}_\alpha$ and $\tilde{w}_\beta$ are independent zero-mean Gaussian distributed random variables with the variances $2N\sigma_w^2/|C|^2$ and $6N\sigma_w^2/|C|^2$, respectively. To facilitate the real part calculation in (9), we express complex valued random variables as the summation of two real valued entities, $\tilde{w}_\alpha = \tilde{w}_{\alpha,r} + j\tilde{w}_{\alpha,i}$ and $\tilde{w}_\beta = \tilde{w}_{\beta,r} + j\tilde{w}_{\beta,i}$. (The introduced real valued random variables have half the variance of their complex valued counterparts.) As SNR increases, the variance of noise terms diminishes and the equation (9) can be approximated with

$$\begin{aligned} \hat{\delta} &\approx c_N(\bar{\delta}_j + \tilde{w}_{\alpha,r} + \bar{\delta}_j\tilde{w}_{\beta,r}) \\ &\approx \bar{\delta}_c + c_N\tilde{w}_{\alpha,r} + \bar{\delta}_c\tilde{w}_{\beta,r}. \end{aligned} \tag{10}$$

The error variance can be written as $\mathrm{var}(\delta - \hat{\delta}) = c_N^2\mathrm{var}(\tilde{w}_{\alpha,r}) + \bar{\delta}_c^2\mathrm{var}(\tilde{w}_{\beta,r}) = c_N^2 N\sigma_w^2/|C|^2 + \bar{\delta}_c^2 3N\sigma_w^2/|C|^2$. This result can be further simplified for small values of δ, by using $\sin(\pi\delta/N) \approx \pi\delta/N$ and $\cos(2\delta\pi/N) \approx 1$ for C given in

(5). With these approximations, $1/|C|^2$ becomes $1/(4A^2N^2)$ and the error variance can be written as

$$\mathrm{var}(\delta-\hat{\delta}) = \frac{c_N^2}{4N\mathrm{SNR}} + \frac{3}{4N\mathrm{SNR}}\bar{\delta}_c^2 \tag{11}$$

where SNR is A^2/σ_w^2.

Comparing the MSE of the estimator with the CR bound given in (3), we see that the MSE of the suggested estimator is $\pi^2/6 \approx 1.65$ times higher than the CR bound at $\delta = 0$. The gap further increases to 2.88 folds at $\delta = 1/2$. This shows that the suggested estimator lacks the statistical efficiency property.

MSE—Gross Error Characterization: Gross errors occur when the peak detected in the first stage is at least two DFT bins away from the true bin, that is when the first stage peak is not under the main-lobe of signal shown in Fig. 1. It can be easily noted that if the peak detected in the first stage has an index $(\hat{k}_p)$ different from k_{p-1}, k_p or k_{p+1}; the final estimation error is guaranteed to be greater than one DFT bin. In this section, we characterize the probability of the gross error event and give an upper bound for the contribution of the gross errors to the overall MSE.

The magnitude of the signal term at the true bin (bin indexed with k_p in Fig. 1) is $s_t = NAe^{j\phi}f(\delta)$, where δ is the fractional part of the true frequency and $f(\alpha) = \frac{1}{N}\sum_{n=0}^{N-1} e^{j\frac{2\pi}{N}\alpha n}$. The signal term for the DFT bins that can possibly cause a gross error is $s_l = NAe^{j\phi}f(\delta+l)$. Here, $2 \le |l| \le N/2$ denotes the DFT bin offset from the true bin.

In the presence of noise, the signal at the true bin becomes a complex Gaussian distributed random variable with mean s_t and variance $N\sigma_w^2$, $b_t \sim \mathcal{CN}(s_t, N\sigma_w^2)$. Similarly, the bins that can cause a gross error have the distribution of $b_l \sim \mathcal{CN}(s_l, N\sigma_w^2)$. A gross error occurs when $|b_l| > |b_t|$. Following ([5], p. 619), we call this event as anomaly and denote its probability as $P_A^l = P\{|b_l| > |b_t|\}$.

The identical anomaly event also appears in the analysis of non-coherent and differentially coherent communication systems, ([6], Appendix B) and its probability can be expressed using ([7], eq. (14)) and ([8] eq. (10)) as follows:

$$P_A^l = Q(\sqrt{U-V}, \sqrt{U+V}) - \frac{1}{2}\exp(-U)I_0(W) \tag{12}$$

$$= \frac{1}{2\pi}\int_0^{\pi} \exp\left(-\frac{V^2}{U - W\cos(\phi)}\right) d\phi \tag{13}$$

where $Q(\cdot,\cdot)$ is the Marcum-Q function, $I_0(\cdot)$ is the modified Bessel function of the first kind and

$$U = \frac{|s_t|^2 + |s_l|^2}{2N\sigma_w^2} = N\mathrm{SNR}\frac{|f(\delta)|^2 + |f(\delta+l)|^2}{2} \tag{14}$$

$$V = \frac{|s_t|^2 - |s_l|^2}{2N\sigma_w^2} = N\mathrm{SNR}\frac{|f(\delta)|^2 - |f(\delta+l)|^2}{2} \tag{15}$$

$$W = N\mathrm{SNR}|f(\delta)f(\delta+l)|. \tag{16}$$

The integrand in (13) is a monotone increasing function of ϕ with the maximum value of $\exp(-V^2/(U+W))$ at $\phi = \pi$. This fact can be used to upper bound P_A^l with $P_A^l \le 1/2\exp(-V^2/(U+W))$:

$$P_A^l \le \frac{1}{2}\exp\left(-\frac{N\mathrm{SNR}|f(\delta)|^2}{2}\left[1 - \frac{|f(\delta+l)|}{|f(\delta)|}\right]^2\right). \tag{17}$$

Examining the last relation, it can be recognized that $\mathrm{SNR}_{k_p} = N\mathrm{SNR}|f(\delta)|^2$ is the SNR at the true DFT bin and the $r_{l\to p} = |f(\delta+l)|/|f(\delta)|$ is the ratio of sidelobe level l to the peak level in the magnitude spectrum, (also see Fig. 1). With these definitions, P_A^l can be expressed as $P_A^l \le 1/2\exp(-\mathrm{SNR}_{k_p}(1 - r_{l\to p})^2/2)$.

As expected, an increase in the value of $r_{l\to p}$ increases the probability of anomaly. We denote the maximum of $r_{l\to p}(2 \le |l| \le N/2)$ with $r_{l\to p}^{\max}$, and upper bound the anomaly probability with $P_A^l \le P_A^{\mathrm{bound}} = 1/2\exp(-\mathrm{SNR}_{k_p}(1 - r_{l\to p}^{\max})^2/2)$.

The contribution of an anomaly event caused by the lth sidelobe to the overall MSE can be (roughly) written as l^2 times the probability of that bin being the maxima found in the first stage. Hence, this contribution is upper bounded by $l^2P_A^l$.

The MSE due to all anomalous events (MSE_A) becomes

$$\mathrm{MSE}_A < \sum_{|l|=2}^{N/2} l^2 P_A^l < 2\sum_{l=2}^{N/2} l^2 P_A^{\mathrm{bound}}. \tag{18}$$

Approximating $2\sum_{l=2}^{N/2} l^2$ with the highest order term in N, which is $N^3/12$, MSE_A can be written as follows:

$$\mathrm{MSE}_A < \frac{N^3}{12}\exp\left(-\frac{\mathrm{SNR}_{k_p}}{2}\left(1 - r_{l\to p}^{\max}\right)^2\right) \tag{19}$$

Note that, the derivation of the bound for MSE_A includes a number of approximations such as neglecting the fractional part of frequency estimation error and approximating the sum $2\sum_{l=2}^{N/2} l^2$ with $N^3/12$. These "rough" approximations only effect the constant scaling term, which is the term of $N^3/12$ in (19). The scaling term has limited influence on the final results, since the bound in (19) is exponentially tight in SNR.

SNR Value For Which MSE Tracks Cramer–Rao Bound: A major goal in the estimator analysis is to find the SNR threshold guaranteeing the fine error operation. At an arbitrary SNR value, both fine-errors and gross-errors contribute to the MSE. For sufficiently high SNR, the MSE is dominated by fine-errors and its value is given by (11). To estimate the SNR threshold, we find the SNR value for which the MSE due to gross errors are on the same order with the fine errors. To this aim, we simply equate the bound for MSE_A in (19), to the fine error MSE in (11) and get the following relation:

$$\frac{c_N^2 + 3\bar{\delta}_c^2}{4N\mathrm{SNR}_T^{cr}} = \frac{N^3}{12}\exp\left(-\frac{N\mathrm{SNR}_T^{cr}|f(\delta)|^2}{2}\left(1 - r_{l\to p}^{\max}\right)^2\right). \tag{20}$$

The SNR_T^{cr} satisfying (20) is denoted as the SNR threshold above which a "good" performance (fine error region) is guaranteed.

Improved Estimator Through Bias Removal: From (10), the bias of the estimator at high SNR can be written as $\delta - \frac{\tan(\pi\delta/N)}{\pi/N}$. Bias becomes the dominant term contributing to the MSE when SNR exceeds SNR_T^b given in (8). To improve the performance at high SNR, that is when $\mathrm{SNR} > \mathrm{SNR}_T^b$; we suggest to apply the inverse function of $f(z) = \frac{\tan(\pi z/N)}{\pi/N}$ to the estimate produced by (1), that is

$$\hat{\hat{\delta}} = \frac{\tan^{-1}\left(\frac{\pi}{N}\hat{\delta}\right)}{\frac{\pi}{N}} = \hat{\delta} - \left(\frac{\pi}{N}\right)^2\frac{(\hat{\delta})^3}{3} + \left(\frac{\pi}{N}\right)^4\frac{(\hat{\delta})^5}{5} + \ldots \tag{21}$$

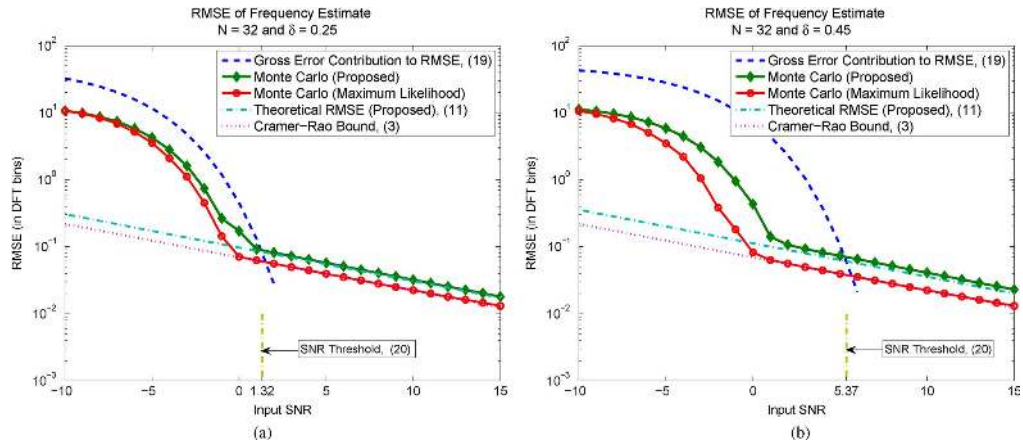

Fig. 2. Comparison of the suggested scheme with the maximum likelihood method and the Cramer–Rao bound. (a) $\delta = 0.25, N = 32$, (b) $\delta = 0.45, N = 32$.

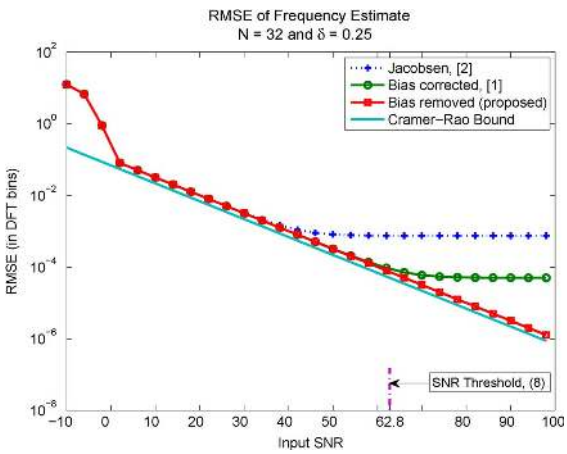

Fig. 3. Comparison of different estimators and the Cramer–Rao lower bound for a wider SNR range than the one given in Fig. 2(a).

The estimate $\hat{\hat{\delta}}$ is unbiased at high SNR and has the error variance relation identical to the one of $\hat{\delta}$ given by (11). We call the estimate $\hat{\hat{\delta}}$ as the bias-removed estimate.

IV. Numerical Results

Fig. 2 shows the results of Monte Carlo runs for two different frequencies at the sample size of $N = 32$. Fig. 2(a) shows the results when the true frequency has an offset of $\delta = 0.25$ bin from a particular DFT bin. We can note that the fine error region of Monte Carlo runs are in close agreement with the analytical result of (11). Furthermore, the SNR threshold, which is the intersection point of the gross error contribution (dashed blue curve) and theoretical RMSE result (cyan dashed line) given by (20), closely matches the threshold observed in the Monte Carlo runs. In comparison to the ML method, the SNR threshold of the examined method is 2 dB higher.

Fig. 2(b) repeats the same comparisons for $\delta = 0.45$. As $|\delta| \to 1/2$, small δ assumption utilized in the analysis starts to depreciate. It can be noted that the analytical prediction for the SNR threshold is 3 dB higher than the actual threshold for this case. It should be remembered that SNR_T^{cr} satisfying (20) is a bound guaranteeing good operation when $\mathrm{SNR} > \mathrm{SNR}_T^{cr}$. Hence, this bound presents a sufficiency condition which gets looser as $|\delta| \to 1/2$.

Fig. 3 presents the results of the simulation given in Fig. 2(a) for a wider range of SNR values. As expected, the suggested bias removal operation through (21) becomes important when SNR exceeds SNR_T^b threshold given in (8). For many applications, SNR_T^b threshold, which is 62.8 dB for the case shown in Fig. 3, is too large to be exceeded. For such applications, the bias-corrected $(\hat{\delta})$ and the bias-removed $(\hat{\hat{\delta}})$ estimates are almost identical.

V. Conclusion

This letter gives a detailed MSE analysis of the estimator suggested in [1] and presents a further improvement shown to be effective at high SNR. The presented results encourage the usage of the suggested method and its variations, such as [9], in practical applications. Last but not the least, we would like to note that the approach for threshold calculation can be applied to study the threshold behaviour of other non-linear parameter estimation problems, [10].

References

[1] C. Candan, "A method for fine resolution frequency estimation from three DFT samples," *IEEE Signal Process. Lett.*, vol. 18, no. 6, pp. 351–354, 2011.

[2] E. Jacobsen and P. Kootsookos, "Fast, accurate frequency estimators," *IEEE Signal Process. Mag.*, vol. 24, no. 3, pp. 123–125, May 2007.

[3] S. M. Kay, *Fundamentals of Statistical Signal Processing, Volume 1: Estimation Theory*. Upper Saddle River, NJ, USA: Prentice-Hall, 1993.

[4] H. L. V. Trees and K. L. Bell, *Bayesian Bounds for Parameter Estimation and Nonlinear Filtering/Tracking*. Piscataway, NJ, USA: Wiley-IEEE Press, 2007.

[5] J. M. Wozencraft and I. M. Jacobs, *Principles of Communication Engineering*. New York, NY, USA: Wiley, 1965.

[6] J. G. Proakis, *Digital Communications*, 4th ed. New York, NY, USA: McGraw-Hill, 2001.

[7] M. K. Simon, "A new twist on the Marcum Q-function and its application," *IEEE Commun. Lett.*, vol. 2, no. 2, pp. 39–41, 1998.

[8] R. Pawula, "A new formula for MDPSK symbol error probability," *IEEE Commun. Lett.*, vol. 2, no. 10, pp. 271–272, 1998.

[9] J.-R. Liao and C.-M. Chen, "Phase correction of discrete Fourier transform coefficients to reduce frequency estimation bias of single tone complex sinusoid," *Signal Process.* vol. X, no. X, pp. X–X, June 2013 [Online]. Available: URL=http://dx.doi.org/10.1016/j.sigpro.2013.05.021, (in print)

[10] F. Athley, "Threshold region performance of maximum likelihood direction of arrival estimators," *IEEE Trans. Signal Process.*, vol. 53, no. 4, pp. 1359–1373, 2005.